MHD Free Convective Heat and Mass Transfer of a Micropolar Fluid Flow over a Stretching Permeable Sheet with Constant Heat and Mass Flux

E. O. Fatunmbi[1], A.S. Odesola[2].
[1]Department of Mathematics and Statistics, Federal Polytechnic, Ilaro, Ogun State, Nigeria.
E-mail: olusojiephesus@yahoo.com
[2]Department of Mathematics, University of Lagos, Akoka, Lagos State, Nigeria.
E-mail: sotontop@yahoo.com

Abstract
This study investigates heat and mass transfer in magnetohydrodynamic micropolar fluid flow past a vertical stretching permeable sheet in a porous medium with constant heat and mass fluxes. A magnetic field of uniform strength is applied normal to the stretching sheet, the governing partial differential equations are transformed into nonlinear coupled differential equations using similarity transformation. The resulting equations are solved by Runge-Kutta method alongside shooting method. The effects of various embedded flow parameters such as magnetic parameter, Soret and Dufour effects, thermal radiation, Prandtl, Schmidt and Eckert numbers, micropolar (material) parameter, suction/injection and permeability are found on velocity, temperature, concentration and microrotation profiles. The influence of the flow parameters on the Skin friction, wall couple shear stress, Nusselt and Sherwood numbers are also obtained and presented in tables. In addition, it was found that micropolar fluid exhibits a reduction in shear stresses as compared to Newtonian fluids
Keywords: Stretching sheet; non-Newtonian fluid; magnetohydrodynamic; micropolar fluid; permeable sheet

1. Introduction
Eringen (1966, 1972) developed the theory of micropolar fluids and as well derived the constitutive equations for the theory of thermo-micropolar fluids. Micropolar fluids are fluids with dilute suspensions of rigid micro-particles with individual motions that support stress and body moments which constitutes a substantial generalization of the Navier-Stokes model and opens up a new field, of potential applications. Micropolar fluid theory is capable of describing complex rheological behaviour of fluids and provides a good mathematical model for some natural and industrial fluids such as polymeric fluids, biological fluids, particles suspension, animal blood and exotic lubricants which cannot be adequately described by the classical Navier-stokes theory. Its applications in a number of industrial processes, such as extrusion of polymer, the flow of exotic lubricants, colloidal suspensions and the cooling of metallic plate in water bath have also boosted the interest of researchers in studying it (Rahman, 2009). A detailed review, on the theory and applications of micropolar fluids, was given by Lukaszewicz (1999) where micropolar fluids

were described as having a complex nature and individual fluid particles may be of different shapes and may shrink and/or expand, occasionally changing shapes and rotating independently of the rotational movement of the fluid. The boundary layer flow of such fluids was first studied by Peddieson and McNitt (1970) and Wilson (1970).

The flow and heat transfer over stretching surfaces has useful and practical applications in engineering activities such as extrusion of plastic sheet, glass blowing, textile and paper production. Similarly, the study of magnetohydrodynamics (MHD) heat and mass transfer over stretching surfaces has found applications in engineering processes such as hot rolling, the extrusion of polymer sheet from a die, the cooling of metallic sheets and a lots more. In such processes, the properties of the final products depend on the kinematic of stretching and the rate of cooling. The rate of cooling can be controlled by drawing the sheets in an electrically conducting fluid subjected to a magnetic field. Crane (1970), pioneered work on stretching sheet, Gupta and Gupta (1977) extended the work to include heat and mass transfer on stretching sheet with suction or blowing. Many other researchers (Grubka and Bobba, 1985; Elbashbeshy, 1998; Quasim *et al.*, 2013) have also investigated fluid flows past stretching surfaces.

The study of heat and mass transfer analysis with chemical reaction, heat generation/absorption in the boundary layer flow is of practical importance due their importance in chemical processes and hydrometallurgical industries, for instance, food processing, manufacturing of ceramics and polymer production (Das, 2012; Mishra *et al.*, 2016). Heat generation/absorption influence may change the temperature distribution of the fluid flow and in consequence affect various engineering devices. To this end, Krishna and Reddy (2018) discussed the unsteady MHD free convection in a boundary layer flow of an electrically conducting fluid through porous medium subject to uniform transverse magnetic field over a moving infinite vertical plate in the presence of heat source and chemical reaction. Krishna and Reddy, (2018) have investigated the simulation on the MHD forced convective flow through stumpy permeable porous medium (oil sands, sand) using Lattice Boltzmann method. Krishna and Jyothi (2017) examined the Hall effects on MHD Rotating flow of a visco-elastic fluid through a porous medium over an infinite oscillating porous plate with heat source and chemical reaction. Similarly, Srinivasacharya and Mendu (2014) studied free convection in MHD micropolar fluid with radiation and chemical reaction effects. Bhattacharyya and Layek (2012) studied MHD boundary layer flow with diffusion and chemical reaction over a porous flat plate with suction/blowing. Mohammed and Abo-Dahab (2009) examined heat and mass transfer in MHD micropolar flow over a vertical moving porous plate in a porous medium with heat generation using perturbation technique.

The aim of the present work is to investigate free convection heat and mass transfer of an electrically conducting non-Newtonian micropolar fluid flow over a stretching permeable sheet with constant heat and mass flux in a saturated Darcy-Forchheimer porous medium. The influences of radiation, viscous dissipation, heat source and chemical reac-

2

tion are also considered. The system of partial differential equations governing the fluid flow is transformed into coupled nonlinear ordinary equations by similarity transformations and the resulting equations are numerically solved by shooting method alongside fourth order Runge-Kutta method.

2. Formulation of the Problem

Consider a steady, two dimensional flow of viscous, incompressible free convective, electrically and thermally radiating and electrically conducting micropolar fluid over a stretching permeable plate in a saturated Darcy-Forchheimer porous medium. A uniform magnetic field of strength B_o is applied normal to the direction of flow in which (x, y) describes the stretching and the transverse coordinates with corresponding velocity component (u, v). The constant heat flux $(-k\frac{\partial T}{\partial y}) = A$ and the constant mass flux $(-Dm\frac{\partial C}{\partial y}) = B$ are considered and the uniform plate temperature $T_w > T_\infty$, where T_∞ is the free stream temperature. The fluid stretching velocity u_w is assumed to vary proportional to the distance x i.e. $u_w = ax$, where a is positive constant. All the fluid properties are isotropic and constant except the density variation with temperature and concentration in the body force term which is approximated by Boussinesq approximation.
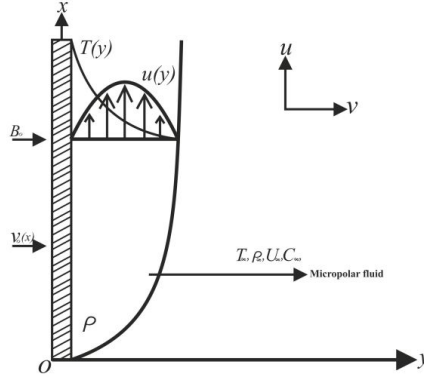

Fig. 1 physical model and coordinate system

Under the above assumptions, the boundary layer and invoking the Boussinesq approximations, the governing equations of continuity, momentum, microrotation, energy and concentration of the fluid flow are respectively given as:

$$\frac{\partial u}{\partial x} + \frac{\partial v}{\partial y} = 0, \tag{1}$$

$$u\frac{\partial u}{\partial x} + v\frac{\partial u}{\partial y} = \frac{(\mu + \kappa)}{\rho}\frac{\partial^2 u}{\partial y^2} + \frac{\kappa}{\rho}\frac{\partial N}{\partial y} + g\beta_T (T - T_\infty) + g\beta_c (C - C_\infty) - \frac{\sigma B_o^2}{\rho}u - \frac{\nu}{K_p}u - \frac{F}{K_p}u^2, \tag{2}$$

$$u\frac{\partial N}{\partial x} + v\frac{\partial N}{\partial y} = \frac{\gamma}{\rho j}\frac{\partial^2 N}{\partial y^2} - \frac{\kappa}{\rho j}\left(2N + \frac{\partial u}{\partial y}\right), \tag{3}$$

3

$$u\frac{\partial T}{\partial x} + v\frac{\partial T}{\partial y} = \frac{k}{\rho C_p}\frac{\partial^2 T}{\partial y^2} + \frac{(\mu + \kappa)}{\rho C_p}\left(\frac{\partial u}{\partial y}\right)^2 - \frac{1}{\rho C_p}\frac{\partial q_r}{\partial y} + \frac{q}{\rho c_p}\left(T - T_\infty\right) + \frac{D_m K_T}{C s C_p}\frac{\partial^2 C}{\partial y^2}, \quad (4)$$

$$u\frac{\partial C}{\partial x} + v\frac{\partial C}{\partial y} = Dm\frac{\partial^2 C}{\partial y^2} + \frac{D_m k_T}{T_m}\frac{\partial^2 T}{\partial y^2} - k_r\left(C - C_\infty\right). \quad (5)$$

The boundary conditions are as follows:

$$u = u_w = ax, v = v_w, N = -m\frac{\partial u}{\partial y}, -k\frac{\partial T}{\partial y} = A, -Dm\frac{\partial C}{\partial y} = B \quad at \ y = 0,$$

$$u \longrightarrow 0, N \longrightarrow 0, T \longrightarrow T_\infty, C \longrightarrow C_\infty \quad as \ \ y \to \infty. \quad (6)$$

Here, $\mu, \nu, \rho, \kappa, j, \gamma$ and v_w, are dynamic viscosity, kinematic viscosity, fluid density, vortex viscosity, micro inertial per unit mass, spin gradient viscosity and suction/injection term. Similarly, T, C, N, k, B_o and K_p are the fluid temperature, fluid concentration, component of microrotation vector normal to x, y plane, thermal conductivity, magnetic field intensity and permeability of the porous medium. Others are: $k_r, \sigma, C_p, T_\infty, C_\infty, T_m, Dm, q$, A, B and q_r represent rate of chemical reaction, electrical conductivity, specific heat at constant pressure, free stream temperature, and the free steam concentration, mean fluid temperature, molecular diffusivity, volumetric rate of heat generation, constant heat flux per unit area, coefficient of mass flux per unit area and radiative heat flux respectively. Also, $F = F_0 x^{-1}, \beta_T = \beta_0 x^{-1}, \beta_c = \beta_0^\star x^{-1}$ represent Forchheimer constant, coefficient of thermal expansion, coefficient of volumetric expansion, and F_0, β_0 and $\beta_0^\star$ are constants (see Makinde, 2010).

Also, m is a surface boundary parameter with $0 \leq m \leq 1$. The case when $m = 0$ corresponds to $N = 0$, this represents a strong concentration such that the micro-particles close to the wall are unable to rotate. When $m = \frac{1}{2}$, this indicates weak concentration of micro-particles and the vanishing of anti-symmetric part of the stress tensor and the case when $m = 1$ is used for modelling turbulent boundary layer flows (see Peddieson, 1972; Ahmadi, 1976; Jena and Mathur, 1981).
$\gamma = \left(\mu + \frac{\kappa}{2}\right) j$, is the spin gradient viscosity. This assumption has been invoked to allow the field of equations to predict the correct behaviour in the limiting case when the microstructure effects becomes negligible and the total spin N reduces to the angular velocity (Ahmadi, 1976).
Using Rosseland approximation,

$$q_r = -\frac{4\sigma^\star}{3\alpha^\star}\frac{\partial T^4}{\partial \bar{y}}, \quad (7)$$

is the radiative heat flux (Brewster, 1992; Akinbobola and Okoya, 2015).
Where, $\alpha^\star$ is the mean absorption coefficient and $\sigma^\star$ is the Stefan-Boltzman constant. We suppose that there exists sufficiently small temperature difference within the flow, such

that T^4 can be expressed as a linear combination of the temperature. Expanding T^4 in Taylor series about T_∞ to obtain

$$T^4 \approx 4T_\infty^3 T - 3T_\infty^4. \tag{8}$$

Hence,

$$\frac{\partial q_r}{\partial \bar{y}} = -\frac{16\sigma^\star T_\infty^3}{3\alpha^\star} \frac{\partial T^2}{\partial y^2} \tag{9}$$

Introducing the stream function
$\psi(x, y)$ as $u = \frac{\partial \psi}{\partial y}$, $v = -\frac{\partial \psi}{\partial x}$, equation (1) is automatically satisfied.
The following dimensionless variables are substituted into Eqs. (2-6)

$$\psi(x, y) = xf(\eta)(a\nu)^{1/2}, \ \eta = \left(\frac{a}{\nu}\right)^{1/2}, \ N = xg(\eta)\sqrt{\frac{a^3}{\nu}}$$
$$\theta(\eta) = \frac{k(T - T_\infty)}{A}\left(\frac{a}{\nu}\right)^{1/2}, \ \phi(\eta) = \frac{Dm(C - C_\infty)}{B}\left(\frac{a}{\nu}\right)^{1/2}. \tag{10}$$

. The resulting non-linear ODEs are:

$$(1 + K)f''' + ff'' + \lambda^2 + Kg' - (Da + M)f' - (Fs + 1)f'^2 = 0, \tag{11}$$

$$\lambda g'' + fg' - f'g - 2Hg - Hf'' = 0, \tag{12}$$

$$\left(1 + \frac{4}{3}R\right)\theta'' + PrEc(1 + K)f''^2 + Prf\theta' + PrQ\theta + PrDu\phi'' = 0, \tag{13}$$

$$\phi'' + Scf\phi' + ScSr\theta'' - Sc\gamma_1\phi = 0, \tag{14}$$

subject to boundary conditions:

$$\eta = 0 : f' = 1, \ f = fw, \ g = -mf'', \ \theta' = -1, \ \phi' = -1, \tag{15}$$

$$\eta \longrightarrow \infty : f' = \lambda, \ g \longrightarrow 0, \ \theta \longrightarrow 0, \ \phi \longrightarrow 0. \tag{16}$$

Here, prime denotes differentiation with respect to η, $K = \frac{\kappa}{\mu}$ is the material parameter, $fw = -\frac{v_w}{\sqrt{a\nu}}$ with $fw > 0$ as the suction and $fw < 0$ corresponds to injection. $Da = \frac{\nu}{aK_p}$ is the Darcy parameter, $M = \frac{\sigma B_o^2}{a\rho}$ is the Magnetic parameter, $Pr = \frac{\mu Cp}{k}$ is the Prandtl number, $Sc = \frac{\nu}{Dm}$ is the Schmidt number, $Q = \frac{q}{a\rho Cp}$ is the heat generation/absorption parameter, $Fs = \frac{F_0}{K_p}$ is the Forchheimer number, $Gr = g\beta_0\sqrt{\frac{\nu}{a^5}}$ is the thermal Grashof number, $Gc = g\beta_0^\star\sqrt{\frac{\nu}{a^5}}$ is the solutal Grashof number, $\lambda = \frac{\gamma}{\nu\rho j}$ is the spin gradient viscosity parameter, $H = \frac{\kappa}{a\rho j}$ is the vortex viscosity parameter, $Ec = \frac{u^3 k}{AxCp\sqrt{a\nu}}$ is the Eckert number, $R = \frac{4\sigma^\star T_\infty^3}{\alpha^\star k_\infty}$ is the radiation parameter, $Du = \frac{BK_T}{\nu CsCp}\frac{k}{A}$ is the Dufour number, $Sr = \frac{DmK_T}{BT_m}\frac{B}{k}$ is the Soret number and $\gamma_1 = \frac{k_r}{a}$ is the chemical reaction parameter.

Quantities of physical interest

The shear stress at the surface is given as $\tau_w = \left[(\mu + \kappa) \left(\frac{\partial u}{\partial y} \right) + \kappa N \right]_{y=o}$.

The skin friction coefficient is defined as $C_f = \frac{\tau_w}{\rho u_w^2} = \frac{[1 + K(1-m)] f''(0)}{\sqrt{Re_w}}$

where $u_w = ax$ is the characteristics velocity and $Re_w = \frac{u_w x}{\nu}$ is the local Reynolds number.

The wall couple stress is defined as $M_w = \left(\gamma \frac{\partial N}{\partial y} \right)_{y=0} = \mu u_w \left(1 + \frac{K}{2} \right) g'(0)$

The local Nusselt number and the Sherwood number are respectively given as

$$Nu_x = \frac{xA}{k (T_w - T_\infty)}, \tag{17}$$

$$Sh_x = \frac{xB}{k (C_w - C_\infty)}, \tag{18}$$

where A and B are respectively given as $A = -k \left[\frac{\partial T}{\partial y} \right]_{y=0}$, $B = -Dm \left[\frac{\partial C}{\partial y} \right]_{y=0}$, using (10) in (17) and (18) gives $Re_x^{-1/2} Nu_x = \frac{1}{\theta(0)}$ and $Re_x^{-1/2} Sh_x = \frac{1}{\phi(0)}$

3. Method of solution

The system of non-linear ordinary differential equations $(11 - 14)$ with the boundary conditions $(15 - 16)$ were solved numerically using Fourth order Runge-Kutta integration scheme alongside shooting method. Systematic estimate of $f''(0)$ and $\theta(0)$ were carried out with shooting technique until the boundary conditions at infinity decay exponentially to zero. The iteration process is repeated until the convergence criterion for all the variables at 10^{-8} is achieved. The step size $\nabla \eta = 0.001$ is used for the numerical solution and the boundary condition $\eta \longrightarrow \infty$ is approximated by $\eta_{max} = 10$.

4. Results and Discussion

To have a clear insight into the behaviour of each of the flow parameters on the physical problem, the computational analysis are carried out for the dimensionless velocity, temperature, concentration and microrotation. The default values of the computation are as follows: $M = 0.5$, $K = 0.5$, $Ec = 0.01$, $Pr = 0.71$, $Sc = 0.22$, $R = 0.2$, $\lambda = 2$, $Da = 0.5$, $Fs = 0.5$, $Q = 0.5$, $m = 0.5$, and $fw = 0.5$, $Sr = 1$, $Du = 0.2$, $Gr = 4$, $Gc = 2$. The plotted graphs correspond to these values unless otherwise indicated on the graph.

To authenticate our numerical analysis, a comparison of the values of the surface temperature $\theta(0)$ for various values of Prandtl number Pr has been made with existing work in literature under some limiting cases and found to be in excellent agreement as shown in Table 1.

Table 1: Comparison of the values of surface temperature $\theta(0)$ with existing works for different values of Pr when
$K = M = R = Da = Fs = Ec = Q = Sc = Du = Sr = \gamma_1 = H = 0$

Pr	Salleh *et al.* (2010)	Qasim *et al.* (2013)	Present results
0.72	-	2.15916	2.15707
1.00	1.71816	1.71816	1.71818
3.00	0.85819	0.85819	0.85819
5.00	0.63773	0.63773	0.63773
7.00	0.52759	0.52758	0.52759
10.00	0.43327	0.43327	0.43328
100.00	0.12877	0.12877	0.12877

Table 2 shows the numerical values of skin friction coefficient, Nusselt number, Sherwood number and the wall couple stress for some pertinent parameters. From this table, it is seen that the material parameter K, the Magnetic parameter M and Forchheimer parameter Fs cause a reduction in the skin friction coefficient, Nusselt number, Sherwood number and the wall couple stress. On the other hand, the skin friction coefficient, wall couple stress and the sherwood number increases with heat generation parameter Q and Dufour parameter Du.

Table 2: Values of $f''(0)$, $\frac{1}{\theta(0)}$, $\frac{1}{\phi(0)}$ and $g'(0)$ for variations in K, M, Fs, Q, fw, Du and γ_1

K	M	Fs	Q	fw	Du	γ_1	$f''(0)$	$1/\theta(0)$	$1/\phi(0)$	$g'(0)$
0.00							1.602837	0.539383	1.071818	1.088777
0.75	0.5	0.5	0.5	0.2	0.5	0.2	1.148439	0.537536	1.069651	0.987890
2.00							0.900419	0.532433	1.064202	0.781472
0.5	0.00						1.767453	0.554924	1.084236	1.198142
	1.50						1.310287	0.510971	1.050286	0.895471
	3.5						0.832752	0.462838	1.017619	0.591926
	0.5	0.5					2.309064	0.414462	1.095415	1.395224
		1.5					1.973539	0.386096	1.081265	1.181854
		2.5					1.711728	0.363254	1.072580	1.020244
			0.1				1.089493	0.681017	0.975858	0.754021
			0.35				1.382569	0.592628	1.029425	0.942556
			0.75				2.062246	0.452645	1.167758	1.399672
			0.5	-0.5			3.083214	0.315423	1.177637	1.692487
				-0.2			2.609241	0.371884	1.114698	1.514225
				0.2			2.019750	0.461203	1.080304	1.274631
				0.2	0.2		1.602837	0.539384	1.0718180	1.087776
					1.0		2.520743	0.377711	1.2952781	1.720463
					0.5	0.5	1.602837	0.538394	1.0718182	1.087776
						1.0	1.568575	0.535830	1.0718185	1.065148

Figs. 2-3 respectively describe the impact of magnetic field parameter M on the velocity and temperature profiles. Observation from Fig. 2 reveals that the fluid velocity

and the velocity boundary layer thickness decrease with an increase in the value of the magnetic field parameter M. This physical response shows that the application of the transverse magnetic field in an electrically conducting fluid creates a retarding force known as Lorentz force which acts against the fluid motion and slows it down. In consequence, the micropolar fluid temperature increases as shown in Fig. 3. Fig. 4 shows the variation of the dimensionless velocity with η for various values of material (micropolar) parameter K. It is noticed that the velocity profiles decrease very close to the plate with the velocity of viscous fluid $K = 0$ higher than that of micropolar fluid. However, further away from the plate the fluid velocity increases with an increase in K due to the rising in the momentum boundary layer thickness. In such case, the micropolar fluid velocity is higher than that of viscous fluid ($K = 0$). Fig. 5 shows that the microrotation profiles rises near the plate and it is negative. The negative values of the microrotation indicate a reverse spinning of the micro-particles.
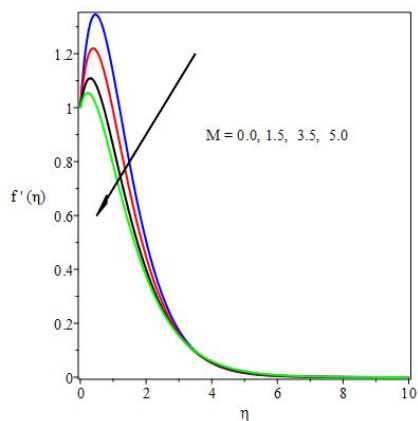
Fig. 2. Effect of M on Velocity profiles   **Fig. 3.** Effect of M on Temperature
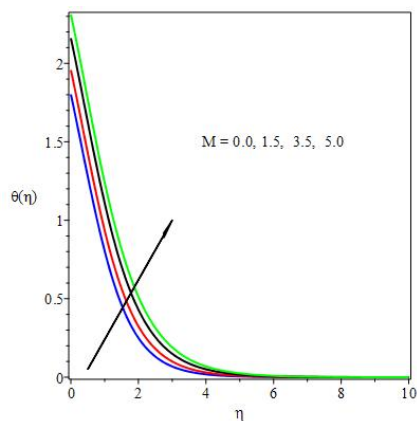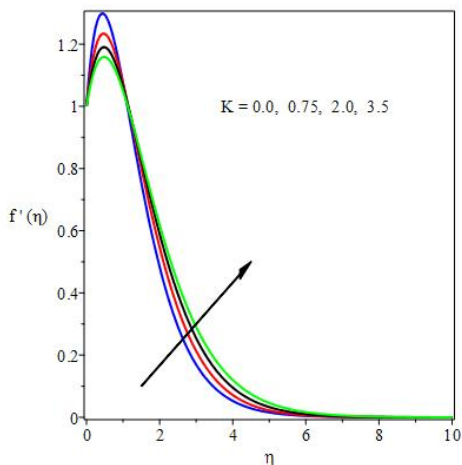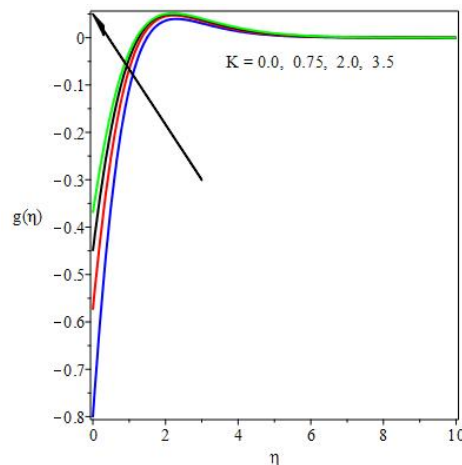

Fig. 4. Effect of K on Velocity   **Fig. 5**. Effect of K on Microrotation profiles

8

Figs. 6-7 describe the influence of Forchheimer Fs on velocity and temperature profiles. As Forchheimer Fs increases, the velocity distribution in the boundary layers decreases due to the tightness of the porous medium, also the hydrodynamic boundary layer thickness decreases as shown in Fig.7, a similar effect happens in the case of the Darcy parameter Da. The resistance to the fluid motion created by the porous medium causes the fluid to heat up leading to a rise in thermal boundary layer thickness and as a result the temperature rises as depicted in Fig. 7. Fig. 8 displays the effect of the radiation parameter R on the temperature distributions. Observation shows that an increase in R has the tendency to enhance the conduction effect and increase temperature at every point away from the surface, in terms of the boundary layer, the thickness of the thermal boundary layer rises as R increases. Hence, to have the cooling at a faster rate R should be reduced. Fig. 9. is a plot of temperature against η for different values of heat generation parameter Q. Heat generation enhances temperature distribution across the boundary layer.
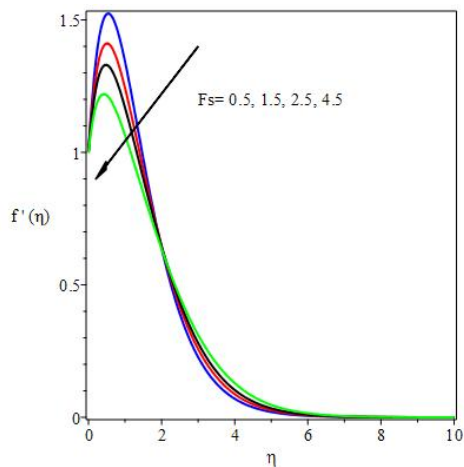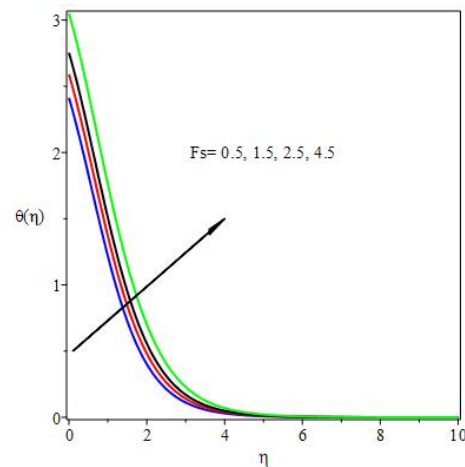

Fig. 6. Effect of Fs on Velocity profiles

Fig. 7. Effect of Fs on Temperature profiles
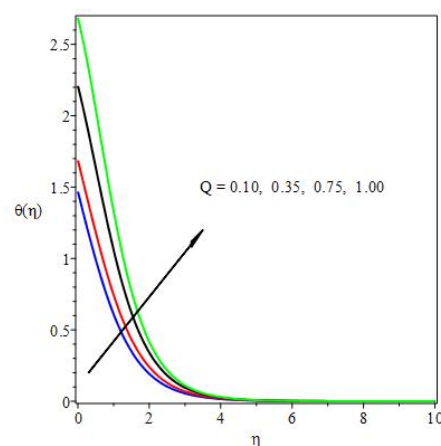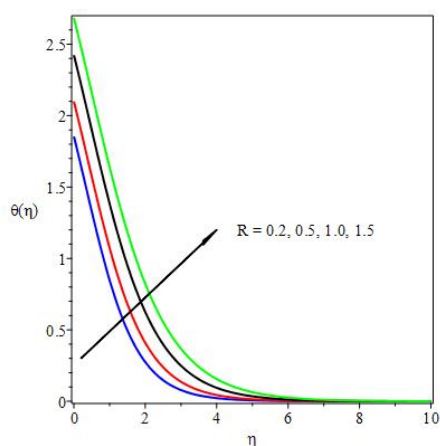
Fig. 8. Effect of R on Temperature   **Fig. 9**. Effect of R on Temperature profiles

Figs.10-11 display the influence of suction/injection fw on velocity and temperature distributions across the boundary layer. Observation shows that both the hydrodynamic and thermal boundary layers fall with an increase in the suction velocity ($fw > 0$). In addition, suction produces a damping effect on the fluid flow due to the fact that the heated fluid is being pushed towards the plate such that the buoyancy force acted to resist the fluid as a result of high influence of viscosity. On the other hand, an increase in the injection parameter $fw < 0$ enhances velocity distribution within the boundary layer.

Fig. 12 depicts a decrease in the microrotation profiles and a negative rotation of the micro-particles with an increase in the spin gradient viscosity parameter λ. However, when the surface boundary parameter $m = 0$ a case of strong concentration of micro-elements, the microrotation decreases near the plate while it increases further away from the plate and with positive spinning of micro-constituents as demonstrated in Fig. 13.

Fig. 14 shows the influence of vortex viscosity parameter H on the microrotation profiles. There is a rise in the microrotation profiles and a negative rotation of the micro-particles with an increase in the vortex viscosity parameter H. Fig. 15 illustrates the effect of Prandtl number Pr on the temperature profiles. It is evident that increase in the Prandtl number Pr causes a reduction in the temperature profile. An increase in Pr implies reducing thermal boundary layer thickness which in turn lowers the average temperature within the boundary layer. Prandtl parameter Pr can therefore be applied to enhance the rate of cooling as fluids with lower Pr produce higher conductivities and at such heat diffuses speedily away from the heated plate than for higher values of Pr.
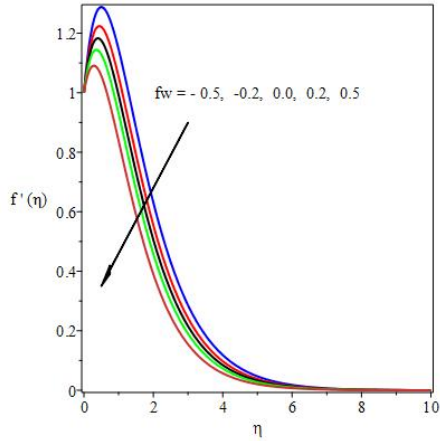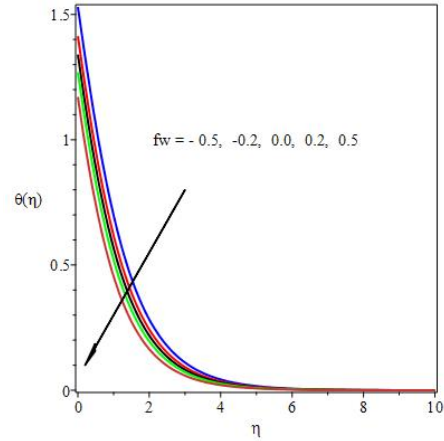

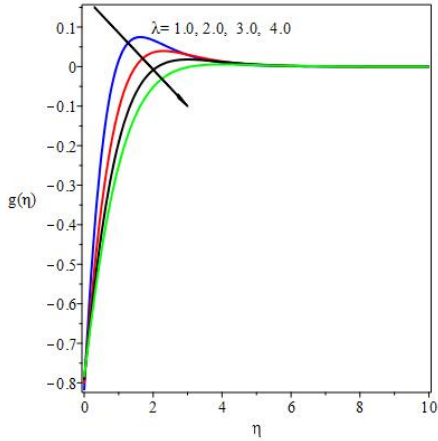**Fig. 10**. Effect of fw on Velocity profiles   **Fig. 11** Effect of fw on Temperature

10

Fig. 12. Effect of λ on Microrotation

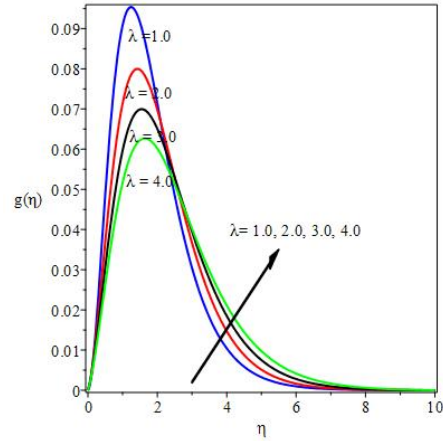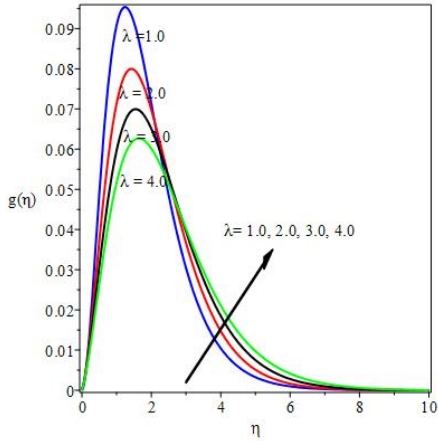**Fig. 13**. Effect of λ on Microrotation profiles @ m=0

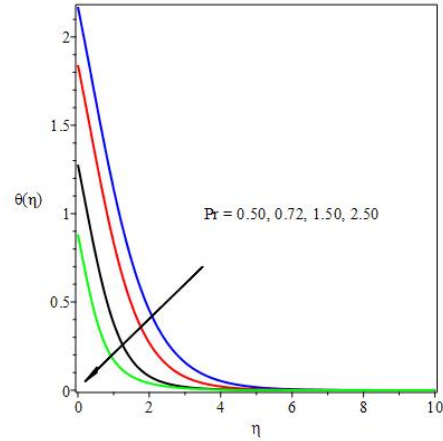
Fig. 14. Effect of H on Microrotation

Fig. 15.Effect of Pr on Temperature

Conclusion

This paper considers the free convective boundary layer flow, heat and mass transfer of an electrically conducting micropolar fluid past a linearly stretching sheet in a saturated Darcy-Forchheimer porous medium with constant heat and mass flux. The governing partial differential equations of the fluid flow are transformed into non-linear coupled ordinary differential equations using an appropriate similarity variables and the resulting equations are solved with the fourth order Runge-Kutta integration scheme coupled shooting method. Comparison of the present results are made with existing work in the literature under some limiting cases and found to be in excellent agreement.

The main observations are:

- An increase in the material (micropolar) parameter K causes a reduction in the skin friction coefficient $f''(0)$, heat transfer $\theta'(0)$, mass transfer $\phi'(0)$ and the wall

11

couple stress $g'(0)$. Thus, the inclusion of micropolar fluid is to reduce the drag along the plate.

- The material (micropolar) parameter K causes a decrease in the fluid velocity close to the plate but increase in fluid velocity further away from the plate, also, an increase in K causes a rise in the microrotation profiles. .

- The heat transfer coefficient increases with increase in suction parameter fw as the skin friction coefficient rises with the Dufour effect.

- The species concentration reduces with an increase in the destructive chemical reaction parameter $\gamma_1 > 0$ parameter, Soret Sr and Schmidt numbers Sc while the trend is reversed for the generative chemical reaction $\gamma_1 < 0$ parameter.

- The momentum boundary layer thickness reduces with an increase in the Darcy Da and Forchheimer Fs parameters while the opposite is the case for thermal boundary layer thickness. The thermal boundary layer thickness diminishes with an increase in the Prandtl number Pr, while the opposite trend is observed with an increase in the radiation parameter R and heat generation parameter Q.

References

Ahmadi, G. (1976). Self-similar solution of incompressible micropolar boundary layer flow over a semi-infinite plate, Int. J. Engng Sci, **14**, 639-646.

Bhattacharyya, K. and Layek, G. C. (2012). Similarity solution of MHD boundary layer flow with diffusion and chemical reaction over a porous flat plate with suction/blowing, *Meccanica* , 47, 1043-1048.

Brewster, M. Q. (1992). *Thermal Radiative Transfer Properties*, Wiley, New York, USA.

Chen, J., Liang, C. and Lee, J. D. (2011). Theory and simulation of micropolar fluid dynamics, *J. Nanoengineering and nanosystems*, **224**, 31-39.

Crane, L. J. (1970). Flow past a stretching plate, *Communicatios Breves*, **21**, 645-647.

Das, K. (2012). Slip effects on heat and mass transfer in MHD microplar fluid flow over an inclined plate with thermal radiation and chemical reaction, *Int. J. Numer. Meth. Fluids*, Doi:10.2002/fd.2683.

Elbashbeshy, E. M. A. (1998). Heat transfer over a stretching surface with variable surface heat flux, *J. Phys. D: Appl. Phys*, 31, 1951-1954.

Eringen, A. C. (1966). Theory of micropolar fluids, *J. Math. Anal. Appl.*, **16**, 1-18.

Eringen, A. C. (1972). Theory of thermo-microfluids,*Journal of Mathematical Analysis and Applications*, **38**, 480-496.

Grubka, L. K. and Bobba, K. M. (1985). Heat and mass transfer characteristics of a stretching surface with variable temperature, *Transactions of the ASME*, **107**, 248-250.

Gupta, P. S. and Gupta, A. S. (1977). Heat and mass transfer on a stretching sheet

with suction or blowing, *Can. J. Chem. Eng.*, **55**, 744-746

Hayat, T., Mustafa, M. and Obaidat, S. (2011). Soret and Dufour effects on the stagnation-point flow of a micropolar fluid toward a stretching sheet, *Journal of Fluid Engineering*, **133**, 1-9.

Hamad, M. A. A., Uddin, M. J, and Ismail, A. I. (2012). Radiation effects on heat and mass transfer in MHD stagnation-point flow over a permeable flat plate with thermal convective surface boundary condition, temperature dependent viscosity and thermal conductivity, *Nuclear Engineering and Design*, **242**, 194-200.

Hayat, T., Shehzda, S. A. and Qasim, M. (2011). Mixed convection flow of a micropolar fluid with radiation and chemical reaction, *Int., Journal for Numerical Methods in Fluids*, **67**, 1418-1436.

Jena, S. K. and Mathur, M. N. (1981). Similarity solutions for laminar free convection flow of a thermomicropolar fluid past a non-isothermal flat plate, Int. J. Eng. Sci. **19**, 1431-1439.

Krishna, M. V., Reddy, G .S. (2018). MHD Forced Convective flow of Non-Newtonian fluid through Stumpy Permeable Porous medium, *Materials Today Proceedings*, **5**, 175183.

Krishna, M. V., Kamboji. J. (2018). Hall effects on MHD Rotating flow of a Visco-elastic Fluid through a Porous medium Over an Infinite Oscillating Porous Plate with Heat source and Chemical reaction, *Materials Today: Proceedings*, 5, 367380.

Krishna, M. V. and Jyotghi, K. (2018). Hall effects on MHD rotating flow of a visco-elastic fluid through a porous medium over an infinite oscillating porous plate with heat source and chemical reaction, *Materials Today: Proceedings*, 5, 367380.

Lukaszewicz, G. (1999). *Micropolar fluids: Theory and Applications* 1st Ed., Birkhauser, Boston.

Mahmoud, M. A. A. (2011). Hydrodynamic stagnation point flow towards a porous stretching sheet with variable surface heat flux in the presence of heat generation, *Chem. Eng. Comm.*, **198**, 837-846.

Makinde, O. D. (2010). Similarity solution of hydromagnetic heat and mass transfer over a vertical plate with a convective surface boundary condition, *Int. Journal of the Physical Sciences*, **5**, 700-710.

Mishra, S .R, Baag, S. and Mohapatra, D. K. (2016). Chemical reaction and Soret effects on hydromagnetic micropolar fluid along a stretching sheet, *Engineering Science and Technology, an International Journal*, **19**, 1919-1928.

Mohamed, R. A. and Abo-Dahab, S. M. (2009). Influence of chemical reaction and thermal radiation on the heat and mass transfer in MHD micropolar flow over a vertical moving porous plate in a porous medium with heat generation, *International Journal of Thermal Sciences*, 48, 1800-1813.

Olajuwon, B. I., Oahimire, J. I. and Waheed, M. A. (2014). Convection heat and mass transfer in a hydromagnetic flow of a micropolar fluid over a

porous medium, *Theoret. Appl. Mech*, 41, 93-117.

Peddieson, J and McNitt, R. P. (1970). Boundary layer theory for micropolar fluid, *Recent Adv. Enggng Sci.*, 5, 405-426.

Peddieson, J. (1972). An application of the micropolar model to the calculation of a turbulent shear flow, *Int. J. Eng. Sci.*, 10, 23-32.

Qasim, M., Khan, I. and Shafle, S. (2013). Heat transfer in a micropolar fluid over a stretching sheet with Newtonian heating, *Plos One*, 8(4), 1-6.

Rahman, M. M. (2009). Convective flows of micropolar fluids from radiate isothermal porous surface with viscous dissipation and joule heating, *Commun Nonlinear Sci. Numer Simulat*, 14, 3018-3030.

Salleh, M.Z, Nazar, R., Pop, I. (2010) Boundary layer flow and heat transfer over a stretching sheet with Newtonian heating, *J. Taiwan Inst Chem Eng* **41**, 651655.

Srinivasacharya, D. and Mendu U. (2014). Free convection in MHD micropolar fluid with radiation and chemical reaction effects, *Chem ind. Chem Eng.*, 20(2), 183-195.

Wilson, A. J. (1970). Boundary layers in micropolar liquids, *Proceedings of Cambridge Philosophical society*, **67**, 469-470.